Article

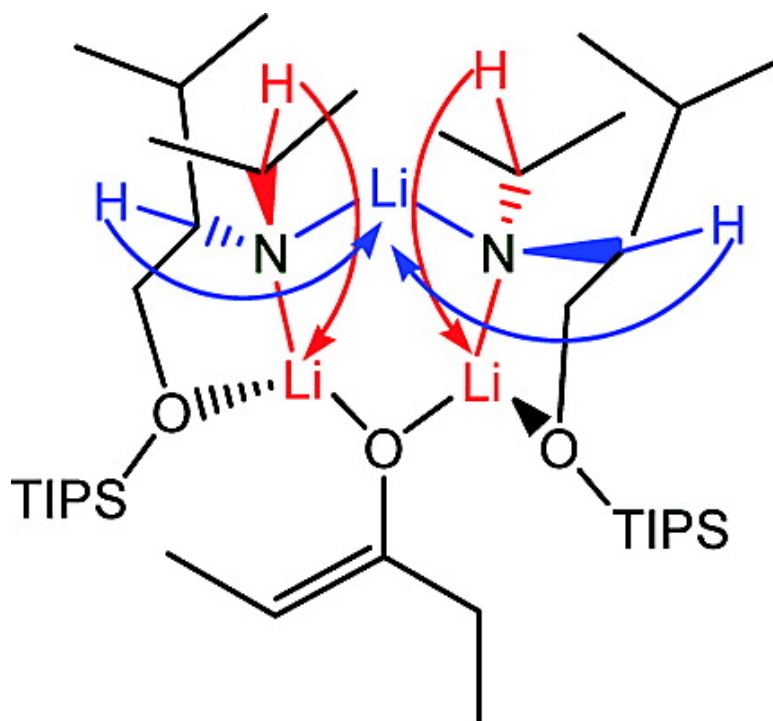# Characterization of a Chiral Enolate Aggregate and Observation of Li#H Scalar Coupling

Deyu Li, Chengzao Sun, and Paul G. Williard

More About This Article

Additional resources and features associated with this article are available within the HTML version:

- Supporting Information
- Access to high resolution figures
- Links to articles and content related to this article
- Copyright permission to reproduce figures and/or text from this article

ACS Publications
High quality. High impact.

Characterization of a Chiral Enolate Aggregate and Observation of ^{6}Li–^{1}H Scalar Coupling

Deyu Li, Chengzao Sun, and Paul G. Williard*

Department of Chemistry, Brown University, Providence, Rhode Island 02912

Received March 21, 2008; E-mail: pgw@brown.edu

Abstract: A chiral enolate aggregate **1** containing a lithium enolate and a chiral lithium amide was systematically investigated by various NMR techniques. ^{1}H and ^{13}C DOSY at 25 and −78 °C provide its solution structure, aggregation number, and formula weight. Multiple 2D ^{6}Li NMR techniques, such as ^{6}Li–^{6}Li EXSY, ^{6}Li–^{1}H HOESY, were utilized to investigate its stereochemical structure. The configuration of the enolate in complex **1** was confirmed by ^{6}Li–^{1}H HOESY and trapping with TMS–Cl. A unique ^{6}Li–^{1}H coupling through the Li–N–C–H network was observed. This scalar coupling was corroborated by ^{6}Li–^{1}H HMQC, deuterium labeling experiments, and selective ^{1}H decoupling ^{6}Li NMR. The stereostructure of **1** provides a model for the origin of enantioselectivity of chiral lithium amide-induced enolate addition reactions.

Introduction

Lithium enolates play a central role in carbon–carbon bond formation reactions and are widely used in organic synthesis.[1] An important aspect of both the formation and the reactivity of lithium enolates is stereoselectivity. While much work related to the diastereoselectivity has been done, much less is known about the enantioselectivity of enolates.[2] The lithium amide effect[3] was invoked to account for enantioselectivity in enolate reactions. This effect arises from mixed aggregates[4] containing both lithium enolates and chiral lithium amides. Thus, identification of the precise solution-state structure of mixed aggregates containing enolate and chiral amide[5] is required to construct a model for probing the origin of the stereoselectivity

in asymmetric enolate reactions involving these complexes.[6] Such models should address the issues of aggregation number, solvation state, and stereochemical structure, all of which are significant factors influencing stereoselective formation and reactivity of the enolate.[1]

In 2000, we published the crystal structure of a mixed aggregate **1** containing 1 equiv of lithium 3-pentanone enolate and 2 equiv of chiral lithium amide **2** derived from (*S*)-*N*-isopropyl-*O*-triisopropylsilyl-valinol **3**[4e] (Scheme 1). This structure represents the first solid-state structure of a mixed aggregate containing a chiral lithium amide base and a lithium enolate anion.[4h,i] We reported only very preliminary NMR results of aggregate **1**, while very little detail is known about the connectivity and stereostructure of this enolate complex. In this Article, we report diffusion-ordered NMR spectroscopy (DOSY) and 1D/2D ^{6}Li NMR studies to determine the detailed stereostructure of complex **1** in solution.

We have previously reported the application of ^{1}H and ^{13}C INEPT DOSY to differentiate dimeric and tetrameric *n*-BuLi,[7]

(1) For leading references, see: (a) Rappoport, Z., Marek, I., Eds. *The Chemistry of Organolithium Compounds*; John Wiley & Sons, Ltd.: New York, 2004. (b) Mahrwald, R., Ed. *Modern Aldol Reactions*; Wiley-VCH Verlag Gmbh & Co.: New York, 2004. (c) Hodgson, D. *Organolithiums in Enantionselective Synthesis*; Springer: New York, 2003. (d) Wu, G.; Huang, M. *Chem. Rev.* **2006**, *106*, 2596–2616. (e) Trost, B. M., Fleming, I., Eds. *Comprehensive Organic Synthesis*; Pergamon: Oxford, 1991.

(2) (a) Uragami, M.; Tomioka, K.; Koga, K. *Tetrahedron: Asymmetry* **1995**, *6*, 701–704. (b) Juaristi, E.; Beck, A. K.; Hansen, J.; Matt, T.; Mukhopadhyay, T.; Simson, M.; Seebach, D. *Synthesis* **1993**, 1271–1290. (c) Muraoka, M.; Kawasaki, H.; Koga, K. *Tetrahedron Lett.* **1988**, *29*, 337–338.

(3) Seebach, D. *Angew. Chem., Int. Ed. Engl.* **1988**, *27*, 1624–1654.

(4) (a) Godenschwager, P. F.; Collum, D. B. *J. Am. Chem. Soc.* **2007**, *129*, 12023–12031. (b) Ramirez, A.; Sun, X. F.; Collum, D. B. *J. Am. Chem. Soc.* **2006**, *128*, 10326–10336. (c) McNeil, A. J.; Toombes, G. E. S.; Chandramouli, S. V.; Vanasse, B. J.; Ayers, T. A.; O'Brien, M. K.; Lobkovsky, E.; Gruner, S. M.; Marohn, J. A.; Collum, D. B. *J. Am. Chem. Soc.* **2004**, *126*, 5938–5939. (d) McNeil, A. J.; Toombes, G. E. S.; Gruner, S. M.; Lobkovsky, E.; Collum, D. B.; Chandramouli, S. V.; Vanasse, B. J.; Ayers, T. A. *J. Am. Chem. Soc.* **2004**, *126*, 16559–16568. (e) Sun, C. Z.; Williard, P. G. *J. Am. Chem. Soc.* **2000**, *122*, 7829–7830. (f) Romesberg, F. E.; Collum, D. B. *J. Am. Chem. Soc.* **1994**, *116*, 9198–9202. (g) Hall, P. L.; Gilchrist, J. H.; Harrison, A. T.; Fuller, D. J.; Collum, D. B. *J. Am. Chem. Soc.* **1991**, *113*, 9575–9585. (h) Williard, P. G.; Hintze, M. J. *J. Am. Chem. Soc.* **1990**, *112*, 8602–8604. (i) Williard, P. G.; Hintze, M. J. *J. Am. Chem. Soc.* **1987**, *109*, 5539–5541.

(5) (a) Shirai, R.; Sato, D.; Aoki, K.; Tanaka, M.; Kawasaki, H.; Koga, K. *Tetrahedron* **1997**, *53*, 5963–5972. (b) Simpkins, N. S. *Pure Appl. Chem.* **1996**, *68*, 691–694. (c) Bambridge, K.; Clark, B. P.; Simpkins, N. S. *J. Chem. Soc., Perkin Trans. 1* **1995**, 2535–2541. (d) Price, D.; Simpkins, N. S. *Tetrahedron Lett.* **1995**, *36*, 6135–6136. (e) Shirai, R.; Aoki, K.; Sato, D.; Kim, H.-D.; Murakata, M.; Yasukata, T.; Koga, K. *Chem. Pharm. Bull.* **1994**, *42*, 690–693. (f) Bunn, B. J.; Simpkins, N. S. *J. Org. Chem.* **1993**, *58*, 533–534. (g) Cain, C. M.; Cousins, R. P. C.; Coumbarides, G.; Simpkins, N. S. *Tetrahedron* **1990**, *46*, 523–544. (h) Cousins, R. P. C.; Simpkins, N. S. *Tetrahedron Lett.* **1989**, *30*, 7241–7244. (i) Simpkins, N. S. *Chem. Ind.* **1988**, 387–389. (j) Simpkins, N. S. *J. Chem. Soc., Chem. Commun.* **1986**, 88–90. (k) Whitesell, J. K.; Felman, S. W. *J. Org. Chem.* **1980**, *45*, 755–756.

(6) (a) Shindo, M.; Koga, K.; Tomioka, K. *J. Org. Chem.* **1998**, *63*, 9351–9357. (b) Fujieda, H.; Kanai, M.; Kambara, T.; Iida, A.; Tomioka, K. *J. Am. Chem. Soc.* **1997**, *119*, 2060–2061. (c) Mulzer, J.; Hiersemann, M.; Bushchmann, J.; Luger, P. *Liebigs Ann. Chem.* **1996**, *5*, 649–654. (d) Galiano-Roth, A. S.; Kim, Y. J.; Gilchrist, J. H.; Harrison, A. T.; Fuller, D. J.; Collum, D. B. *J. Am. Chem. Soc.* **1991**, *113*, 5053–5055.

(7) Keresztes, I.; Williard, P. G. *J. Am. Chem. Soc.* **2000**, *122*, 10228–10229.

Scheme 1[a]

TIPS = triisopropylsilyl
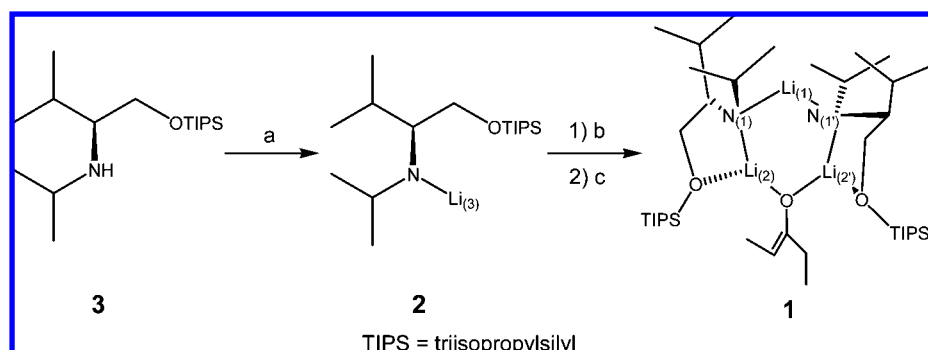
[a] (a) 1.0 equiv of 2.5 M *n*-BuLi in hexanes, toluene-d_8, 0 °C, 5 min; (b) 0.55 equiv of 3-pentanone, 0 °C, 30 min; (c) 0.55 equiv of 2.5 M *n*-BuLi in hexanes, 0 °C.

LDA-THF dimer,[8] mixed alkoxide complex,[9] lithium allylic amide aggregates,[10] and bis(diisopropylamino)boron enolate of *tert*-butyl methyl ketone[11] in solution based on their mobilities. Since our initial reports, DOSY has emerged as a promising technique to study organolithium aggregates as well as other organometallic species, such as magnesium enolates[12] and other transition metal complexes.[13] Hence, DOSY has become the preferred technique for characterizing solvation state and aggregation number of solution-state organometallic complexes in our laboratory.

Because ^{6}Li is a spin 1 nucleus and exhibits a much sharper line width as compared to ^{7}Li, ^{6}Li NMR techniques are preferred to probe the solution structure of organolithium species. However, interpretation of a 1D ^{6}Li NMR is difficult in the absence of 2D experiments due to the limited chemical shift range and different reference standards.[14] For 2D ^{6}Li-related NMR techniques, ^{6}Li—^{6}Li COSY[15] is the basic NMR experiment utilized to assign two or more ^{6}Li peaks to a single aggregate but is usually limited by the small ^{6}Li—^{6}Li coupling constants. ^{6}Li—^{6}Li EXSY[16] provides an alternative method of accomplishing this based on the assumption that ^{6}Li—^{6}Li exchange detected is intramolecular. Other 2D experimental methods applied to organolithium compounds include: ^{6}Li—^{13}C

correlation such as ^{6}Li—^{13}C HETCOR[17] and ^{6}Li—^{13}C HMQC,[18] ^{6}Li—^{1}H NOE such as ^{6}Li—^{1}H HOESY,[19] and ^{6}Li—^{15}N correlation such as ^{6}Li—^{15}N HMQC.[20] We applied the aforementioned DOSY and several 2D ^{6}Li NMR techniques to investigate the solution structure of the mixed lithium aggregate **1**.

During the investigation of aggregate **1** by ^{6}Li NMR at different temperatures, we observed a unique three-bond ^{6}Li—^{1}H scalar coupling. This coupling provides additional stereochemical information for chiral aggregate **1**. The assigned stereochemistry was also confirmed by three methods: ^{6}Li—^{1}H HMQC, deuterium labeling experiments, and selective proton decoupling ^{6}Li NMR.
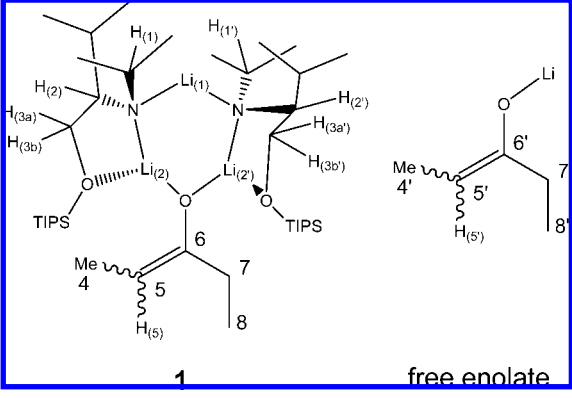
Results and Discussion

Our NMR investigation of complex **1** is composed of two parts. The first part is the characterization of complex **1** by DOSY and 2D ^{6}Li NMR techniques. The observation and identification of the unique three-bond ^{6}Li—^{1}H scalar coupling is presented in the second part.

Part I. Structure Determination of Aggregate 1 by Multiple NMR Techniques. Results of our solution-state structural studies of complex **1** by multiple NMR techniques include three steps. The first step utilizes regular 1D and 2D ^{1}H and ^{13}C NMR techniques to assign the chemical shift to protons and carbons in the aggregate. Internal-reference correlated ^{1}H and ^{13}C INEPT DOSY to determine the formula weight of the complex **1** in solution and corroborate its aggregation state is

(8) Li, D.; Hopson, R.; Li, W.; Liu, J.; Williard, P. G. *Org. Lett.* **2008**, *10*, 909–911.
(9) Liu, J.; Li, D.; Sun, C.; Williard, P. G. *J. Org. Chem.* **2008**, *73*, 4045–4052.
(10) Jacobson, M. A.; Keresztes, I.; Williard, P. G. *J. Am. Chem. Soc.* **2005**, *127*, 4965–4975.
(11) Ma, L.; Hopson, R.; Li, D.; Zhang, Y.; Williard, P. G. *Organometallics* **2007**, *26*, 5834–5839.
(12) He, X. Y.; Morris, J.; Noll, B. C.; Brown, S. N.; Henderson, K. W. *J. Am. Chem. Soc.* **2006**, *128*, 13599–13610.
(13) (a) Megyes, T.; Jude, H.; Grosz, T.; Bako, I.; Radnai, T.; Tarkanyi, G.; Palinkas, G.; Stang, P. J. *J. Am. Chem. Soc.* **2005**, *127*, 10731–10738. (b) Pichota, A.; Pregosin, P. S.; Valentini, M.; Worle, M.; Seebach, D. *Angew. Chem., Int. Ed.* **2000**, *39*, 153–156.
(14) The references of ^{6}Li spectra were chosen arbitrarily by different investigators, and we used external 0.3 M ^{6}LiCl in MeOH-d_4 set at δ 0.0 ppm.
(15) (a) Günther, H.; Eppers, O.; Hausmann, H.; Huels, D.; Mons, H.-E.; Klein, K.-D.; Maercker, A. *Helv. Chim. Acta* **1995**, *78*, 1913–1932. (b) Hilmersson, G.; Davidsson, O. *Organometallics* **1995**, *14*, 912–918. (c) Barr, D.; Clegg, W.; Hodgson, S. M.; Mulvey, R. E.; Reed, D.; Snaith, R.; Wright, D. S. *J. Chem. Soc., Chem. Commun.* **1988**, 367–369. (d) Günther, H.; Moskau, D.; Dujardin, R.; Maercker, A. *Tetrahedron Lett.* **1986**, *27*, 2251–2254.
(16) (a) Meier, B. H.; Ernst, R. R. *J. Am. Chem. Soc.* **1979**, *101*, 6441–6442. (b) Jeener, J.; Meier, B. H.; Bachman, P.; Ernst, R. R. *J. Chem. Phys.* **1979**, *71*, 4546–4553.

(17) Thomas, R. D. In *Isotopes in the Physical and Biomedical Sciences, Vol. II, "Isotopic Applications in NMR Studies"*; Buncel, E., Jones, J. R., Eds.; Elsevier: Amsterdam, 1991; pp 367−410.
(18) (a) Bauer, W. *J. Am. Chem. Soc.* **1996**, *118*, 5450–5455. (b) Gais, H. J.; Vollhardt, J.; Günther, H.; Moskau, D.; Lindner, H. J.; Braun, D. *J. Am. Chem. Soc.* **1988**, *110*, 978–980. (c) Moskau, D.; Brauers, F.; Günther, H.; Maercker, A. *J. Am. Chem. Soc.* **1987**, *109*, 5532–5534.
(19) (a) Gschwind, R. M.; Rajamohanan, P. R.; John, M.; Boche, G. *Organometallics* **2000**, *19*, 2868–2873. (b) Schade, S.; Boche, G. *J. Organomet. Chem.* **1998**, *550*, 381–395. (c) Schade, S.; Boche, G. *J. Organomet. Chem.* **1998**, *550*, 359–379. (d) Bauer, W. *Magn. Reson. Chem.* **1996**, *34*, 532–537. (e) Berger, S.; Mueller, F. *Chem. Ber.* **1995**, *128*, 799–802. (f) Bauer, W.; Lochmann, L. *J. Am. Chem. Soc.* **1992**, *114*, 7482–7489. (g) Hoffmann, D.; Bauer, W.; Schleyer, P. v. R. *J. Chem. Soc., Chem. Commun.* **1990**, 208–211. (h) Bauer, W.; Schleyer, P. v. R. *Magn. Reson. Chem.* **1988**, *26*, 827–833. (i) Bauer, W.; Clark, T.; Schleyer, P. v. R. *J. Am. Chem. Soc.* **1987**, *109*, 970–977. (j) Bauer, W.; Mueller, G.; Pi, R.; Schleyer, P. v. R. *Angew. Chem.* **1986**, *98*, 1130–1132.
(20) (a) Collum, D. B. *Acc. Chem. Res.* **1993**, *26*, 227–234. (b) Gilchrist, J. H.; Harrison, A. T.; Fuller, D. J.; Collum, D. B. *Magn. Reson. Chem.* **1992**, *30*, 855–859.

Table 1. ^{1}H and ^{13}C NMR Signal Assignments of Complex **1** and Free Lithium Enolate

carbon atom	^{13}C	^{1}H
1	51.3	3.07
1′	52.1	3.11
2	68.5	2.78
2′	68.5	2.73
3	68.1/68.0 (*E/Z^a*)	3a: 3.89
		3b: 3.39
3′	67.2	3a′: 4.00
		3b′: 3.43
4	33.7	2.07,2.02 (*E/Z^a*)
5	86.3	4.03
6	162.5	NA
7	33.9	1.71
8	12.6	1.09
4′	32.5	2.14
5′	88.0	4.23
6′	164.0	NA
7′	27.9	1.57
8′	12.6	1.14

^{a} *E/Z* enolate could not be distinguished with these NMR data; detailed studies are presented in the following sections.

in the second step. The last step uses ^{6}Li-related 1D and 2D NMR techniques to investigate connectivity, detailed structural features, and stereochemistry of chiral complex **1**. These results are presented in this order in the following sections.

Step 1. ^{1}H and ^{13}C NMR Assignment of Complex 1. The chiral amino ether ligand **3** is easily synthesized from valinol in two steps.[21] The complete assignments of the proton and ^{13}C signals are summarized in Table S1 (Supporting Information).

A sample of aggregate **1** in toluene-d_8 was generated by slow addition of 3-pentanone to a solution of lithium amide **2** followed by regeneration of the Li-amide as depicted in Scheme 1. ^{1}H NMR, ^{13}C NMR, COSY, HSQC, HMBC experiments of complex **1** were carried out, and the assignment of major proton and ^{13}C signals is summarized in Table 1.

Several structural features need to be emphasized. After 0.55 equiv of 3-pentanone was added to 1.0 equiv of lithium amide **2**, 0.50 equiv of lithium enolate incorporates into the trimeric complex **1**. The remaining 0.05 equiv of lithium enolate exists as a free enolate homoaggregate, and its olefinic proton H$_{(5′)}$ is clearly separated from H$_{(5)}$ of complex **1** in ^{1}H NMR (Table 1). The crystal structure of **1** was refined with a crystallographic C_2 symmetry axis passing through Li$_1$ and the enolate oxygen as depicted in Scheme 1. However, the unsymmetrical nature of the enolate component in this aggregate precludes

existence of a real C_2 symmetry axis in this complex. Hence, we observed that ^{1}H and ^{13}C signals of the left and right lithium amide are different from each other (Table 1). The following chemical shift differences are distinguishable: 1/1′, 2/2′, and 3/3′ (Table 1). Consequently, the stereochemical features of aggregate **1** are subtle.[22] The carbon signal of C5 at 86.3 ppm of the enolate double bond is upfield as compared to regular olefin signals (110−150 ppm). This shielding effect is expected for a simple enolate.[23]

Step 2. ^{1}H and ^{13}C INEPT DOSY Identification of Aggregate 1. DOSY Correlation of Aggregate 1 and Internal References at 25 °C. We first carried out ^{1}H and ^{13}C INEPT DOSY at 25 °C to identify complex **1** in toluene-d_8 solution. To avoid artifacts generated by temperature fluctuation, viscosity change, and convection, we chose 1-tetradecene (TDE), cyclooctene (COE), and benzene[24] as the internal references for the DOSY experiments. The ^{1}H DOSY spectrum of complex **1** with the three internal references in toluene-d_8 solution separates into four components in the diffusion dimension. These are clearly identifiable in the DOSY spectrum reproduced in Figure 1. In increasing order of diffusion coefficient (decreasing formula weight), these are complex **1** ($C_{39}H_{85}Li_3N_2O_3Si_2$, mw 707.1), TDE ($C_{14}H_{28}$, mw 196.4), COE ($C_8H_{14}$, mw 110.2), and benzene (C_6H_6, mw 78.1). The ^{1}H signals of the protons 1, 1′, 2, 2′, 3a, 3a′, 3b, 3b′, and 5 in complex **1** exhibit identical diffusion coefficients.

Because the protons from the enolate anion and lithium amide have identical diffusion coefficients, a question arises from these DOSY results: Is this observation evidence of the existence of complex **1**, or it is a coincidence for the two different complexes, that is, a homolithium amide aggregate and a homolithium enolate aggregate that bear similar diffusion characteristics? Previously, we have suggested a correlation between diffusion coefficient and formula weight utilizing DOSY experiments to

(21) (a) Ohfune, Y.; Kurokawa, N.; Higuchi, N.; Saito, M.; Hashimoto, M.; Tanaka, T. *Chem. Lett.* **1984**, 441–444. (b) Ando, A.; Shioiri, T. *Tetrahedron* **1989**, *45*, 4969–4988.

(22) A perceptive reviewer noted that observation of two sets of chemical shifts for H1/H1′, H2/H2′, and H3a,b/H3a′,b′ and their corresponding carbons is due to atropisomerism. Because the two nitrogen atoms, N1 and N1′, are tetrahedral, they are also stereogenic centers in addition to the two carbon stereogenic centers initially derived from L-valine with *S* configuration. Hence, excluding any consequences of restricted axial rotation about the enolate C−O bond, a total of three different diastereomers of complex **1** are possible, *SRRS*, *SSSS*, and *SRSS* for C2, N1, N1′, C2′, respectively. Because of the unsymmetrical nature of the enolate, all of these isomers exhibit only *C1* point group symmetry overall. Consequently, the H3a,b/H3a′,b′ protons are diastereotopic in all of these isomers when restricted rotation exists. Hence, these four protons along with the H1/H1′ and H2/H2′ protons could have different chemical shifts in all three stereoisomers. Additionally, only the *SRSS* isomer can generate a different stereoisomer, that is, can exhibit atropisomerism, if rotation is restricted about the enolate C−O bond. Generation of a new stereoisomer due to restricted rotation is not possible for the *SRRS* or the *SSSS* isomers. Throughout this article, we have depicted the *SRRS* isomer based upon the X-ray crystal structure determination. We also tend to favor restricted rotation about the C−O enolate bond based upon the steric hindrance due to the TIPS substituents. We understand the term atropisomerism to refer to possibility of new and distinct stereoisomers, that is, either enantiomers or diastereomers. Thus, while there are observable NMR phenomena that arise as a consequence of the stereochemistry and restricted rotation in the *SRRS* isomer that would not be observable in the absence of these features, we do not believe that it is appropriate to utilize the term atropisomerism to refer to this situation within a single stereoisomer. Perhaps atropotopicity rather than atropisomerism is a more appropriate term to describe the NMR spectra of the *SRRS* isomer.

(23) Wen, J. Q.; Grutzner, J. B. *J. Org. Chem.* **1986**, *51*, 4220–4224.

(24) There are three requirements for internal references: (a) they should be inert to the components in solution; (b) the chemical shifts of these internal references should not overlap with the components in solution; and (c) the internal references should have no or little coordinating ability to the complexes in solution.
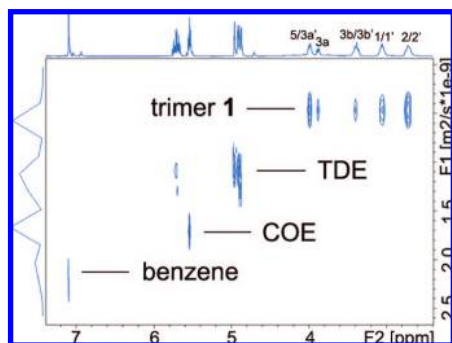
Figure 1. [1]H DOSY of complex **1** and internal references in toluene-d_8 at 25 °C.

study vinylic lithiation of allylamine derivatives.[10] The current ^{1}H DOSY results of complex **1** and the three internal references, TDE, COE, and benzene, can also be utilized to define a linear correlation between the relative log D (diffusion coefficient) and log FW (formula weight). The correlation between log FW and log D of the linear least-squares fit to reference points of all components in this mixture is extremely high, $r = 0.9991$ (Table 2 and Figure 2). [13]C INEPT DOSY shows a similar separation (Figure S17, Supporting Information) and a better log FW and log D correlation ($r = 0.9998$, Table 2 and Figure 2). These remarkable results prove that the existence of complex **1** in solution is valid and not a coincidence from different aggregates.

An added bonus of 2D-[1]H-DOSY spectra is to extract a one-dimensional ^{1}H spectrum slice at the diffusion coefficient of a particular species. To emphasize this point, we have depicted peaks in the slice of complex **1** (Figure 3b) to be compared to the spectrum of the pure, authentic sample (Figure 3b′). The ^{1}H NMR slice taken at the diffusion coefficients of enolate complex **1** agrees very well with its respective ^{1}H NMR spectrum and contains no peaks from a homoenolate aggregate (Table 1). The ^{1}H NMR slices of internal references are also consistent with their authentic ^{1}H NMR spectra. These results support the existence of complex **1** in solution from the chemical shift perspective.

DOSY Correlation of Complex 1 and Internal References at −78 °C. Because it is well-known that organolithium aggregation state is temperature dependent, it is necessary to prove the existence of complex **1** at −78 °C, which is the typical temperature for performing asymmetric aldol reactions. By utilizing the same samples in the above section, DOSY and other NMR experiments were carried out at −78 °C.[25] In both ^{1}H and ^{13}C INEPT DOSY spectra (Figures S23 and S24, Supporting Information), all components were separated very well in the diffusion dimension. The linear least-squares fit of all components in the solution is good: [1]H ($r = 0.9993$) and ^{13}C INEPT ($r = 0.9965$). Hence, these DOSY spectra suggest the same complex **1** exists at low temperature (−78 °C) as well as at room temperature.

In total, four DOSY experiments were carried out for complex **1**. They all showed good separation among different components according to their formula weights. The least-squares fits between log D and log FW are remarkably high (>0.9960), and the average is 0.9987. The high accuracy of all DOSY

correlations indicates the existence of complex **1** and its aggregation state.

Step 3. [6]Li-Related 1D and 2D NMR Investigation of Complex 1. A [6]Li-enriched crystalline complex of **1** was dissolved in toluene-d_8, and the [6]Li NMR spectrum was recorded at −78 °C (Figure 4).[26] This spectrum exhibited three single peaks at δ 3.73, 2.70, and 2.27 ppm. The peak at δ 2.70 ppm was assigned to lithium amide **2**.[27] Integration of the other two singlets at δ 3.73 and 2.27 ppm revealed a 1:2 ratio as expected for complex **1**.

A [6]Li−[6]Li EXSY experiment[16] at 10 °C revealed cross peaks for the two [6]Li peaks at δ 3.73 and 2.27 ppm, strongly indicating that these lithium signals arise from the same complex (Figure 5). These two peaks are assigned to Li$_{(1)}$ and Li$_{(2)/(2')}$, respectively, in complex **1** by comparison with our previous NMR determination of the solution structure of Li-amide/n-BuLi aggregate **4** (Figure 6).[28] The toluene-d_8 solution of complex **1** was stable at −78 °C overnight, but warming it to room temperature resulted in an increase of the Li-amide peak at δ 2.70 ppm and a decrease of the other two peaks, while cooling it back down did not return the original spectrum. However, the ratio of the peaks at δ 3.73 and 2.27 ppm remained at 1:2 as expected. This suggests that either complex **1** at higher temperatures might equilibrate to lithium amide **2** and enolate homoaggregate, or lithium enolate in complex **1** decomposes back to ketone and lithium amide **2** is released from complex **1**.

[6]Li−[6]Li EXSY experiment is a powerful tool for determining lithium atom exchange in solution. It is based on the assumption that at a certain temperature, only intramolecular and not intermolecular exchange is observable on the NMR time scale. Therefore, this experiment can be used to determine whether two lithium signals belong to the same aggregate. Because we observe cross peaks between the two singlets at δ 3.73 and 2.27 ppm and no cross peak to the peak at δ 2.70 ppm, we conclude that the two lithium ions in complex **1** exchange with each other. However, it is possible that the two peaks at δ 3.73 and 2.27 ppm arise from two different aggregates, which, by coincidence, happen to exhibit fast intermolecular Li atom exchange relative to the amide-only aggregate. Previously, we have proven that the solution structure of mixed aggregate **4** exists in solution as the complex depicted in Figure 6.[28] Hence, we chose to determine if [6]Li−[6]Li EXSY cross peaks are observable for the intermolecular exchange of [6]Li between the two similar complexes **1** and **4** containing lithium enolate and n-BuLi, respectively. If intermolecular exchange of [6]Li is observable in the [6]Li−[6]Li EXSY spectrum of a solution containing both complex **1** and **4**, then our assumption based upon observation of the cross peaks in the EXSY spectrum of the aggregate **1** does not necessarily imply that the two peaks belong in the same aggregate. If intermolecular exchange is not observable between complex **4** and **1**, then we can be more confident in concluding that the EXSY cross peaks that we observe represent

(25) One internal reference, TDE, is a liquid at room temperature and crystallizes out from the solution at −78 °C, and most signals of TDE disappeared in ^{13}C INEPT DOSY spectra.

(26) Preparation of complex **1** sample from different methods yielded complex **1** as the major component together with different minor products. That is, by directly mixing 1.0 equiv of lithium amide and 0.55 equiv of lithium enolate, complex **1** coexisted with lithium enolate homo-aggregate. Or if we dissolved crystals of trimer **1** in toluene-d_8, this method yielded a mixture solution containing complex **1** and lithium amide **2**.

(27) The identity of this peak was proved by mixing a stoichiometric amount of ligand **3** and n-Bu[6]Li.

(28) Li, D.; Sun, C; Liu, J.; Hopson, R.; Li, W.; Williard, P. G. *J. Org. Chem.* **2008**, *73*, 2373–2381.

Table 2. log D and log FW Correlation of DOSY Experiments

	log D				
	benzene FW 78.1	COE FW 110.2	TDE FW 196.4	trimer **1** FW 707.1	r (log D − log FW)
[1]H, 25 °C	−8.639	−8.757	−8.892	−9.263	0.9991
INEPT, 25 °C	−8.615	−8.719	−8.867	−9.227	0.9998
[1]H, −78 °C	−9.692	−9.801	−9.952	−10.366	0.9993
INEPT, −78 °C	−9.622	−9.701		−10.756	0.9965

only intraaggregate exchanges. Experimental results reported herein support this latter conclusion.

Samples for NMR containing both complex **1** and **4** were prepared by adding n-Bu^{6}Li into a solution that contained both complexes **1** and **2**. In the ^{6}Li NMR spectrum at 25 °C, the three peaks that appeared in the original sample remained but shifted to δ 3.44, δ 2.47, and δ 1.93 ppm, respectively, due to the temperature increase. Two new peaks appeared at δ 3.58 and δ 2.91 ppm, which were assigned to the aggregate **4** according to our previous observations.[28] The integration ratio of peaks at δ 3.44 and δ 1.93 ppm remained constant at 1:2, as did the peaks at δ 3.58 and δ 2.91 ppm, while integration ratios of the peak at δ 2.47 varied from sample to sample depending upon the quantity of n-Bu^{6}Li added. In this manner, we obtained a solution containing three different aggregates, enolate complex **1**, n-BuLi complex **4**, and lithium amide **2**.

The ^{6}Li−^{6}Li EXSY spectrum of this mixture at 25 °C showed cross peaks only between peaks that we proposed to be in the same aggregate, as depicted in Figure 6. Hence, cross peaks were observable only between peaks at δ 3.44 and δ 1.93 ppm from complex **1** and only between peaks at δ 3.58 and δ 2.91 ppm from the aggregate **4**. Therefore, we conclude that no intermolecular exchange is observable in the ^{6}Li−^{6}Li EXSY spectrum of this solution even between the complexes **4** and **1** with very similar structures. Furthermore, this justifies our conclusion that the two peaks at δ 3.44 and δ 1.93 ppm (or at δ 3.73 and δ 2.27 ppm at −78 °C) belong to the same aggregate, which we assign to the complex **1**, identical to the solid-state structure.

A ^{6}Li−^{1}H HOESY spectrum was obtained at 25 °C to assess the similarity of the stereostructure in solution relative to the solid state through the determination of the hydrogen−lithium atom distances. In Figure 7, we provide the distances found in the solid-state structure of aggregate **1**, and we depict these numbers next to the cross peaks in the corresponding ^{6}Li−^{1}H HOESY spectrum. We were very pleased to find that all of the distinguishable lithium atoms that are close to protons in the solid-state structure exhibited cross peaks in the ^{6}Li−^{1}H HOESY spectrum. These dipolar couplings suggest that the solution structure does not change significantly relative to the solid state.

A structure with some relevant protons shown is given in Scheme 2 for easy interpretation of Figure 7. It is noteworthy
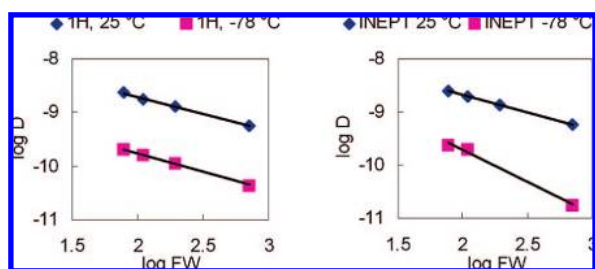
that the observation of a HOESY cross peak between both H$_{(3b)/(3b')}$ and Li$_{(2)/(2')}$ in this spectrum proves the existence of the five-membered chelate ring formed by coordination of the ligand oxygen atoms with lithium atoms. This result also substantiates our previous observation[4i] that silyl ether oxygens are not necessarily poor electron donors.[29] Another important piece of information that we obtained from this HOESY experiment is the observation of the cross peak between the allylic proton H$_{(4)}$ on the enolate with Li$_{(2)/(2')}$. This observation strongly suggests the assignment of the enolate olefin stereochemistry as Z.

One important aspect of the ^{6}Li NMR spectra of solutions containing the aggregate **1** is that sometimes they contain two minor peaks at δ 3.20 and δ 1.79 ppm. We believe that these peaks result from an aggregate similar to complex **1** that incorporates an (E)-enolate because they display nearly identical features in the NMR spectra. The similarities include: an integration ratio of 1:2 between the two peaks, cross peaks from the EXSY spectrum, a triplet and doublet in proton-coupled ^{6}Li NMR spectrum, and the selective proton decoupling patterns.[30] Because the preparation of the NMR samples could not completely separate the crystals from the solution from which they have grown,[31] it was impossible to eliminate all traces of the solution that contains (E)-enolate aggregate. This accounts for the variability in our NMR observations. In previous work, we trapped the enolate aggregate **1** solution (not from dissolving crystal) with TMS−Cl and yielded a mixture of E:Z isomers in a ratio of 32:68.[4e] We will present the detailed identification of the configuration of the enolate double bond in complex **1** in the following section.

Determination of the Stereochemistry of Enolate in Complex 1. The X-ray crystal structure of **1** was refined with a crystallographic 2-fold axis of symmetry. This structure is very similar to the structure of complex **4**.[28] Because the enolate of 3-pentanone cannot by itself possess a 2-fold rotation axis symmetry, the crystallographic model included disorder, which makes it difficult to define the configuration of the enolate.[32]

To determine this stereochemistry unambiguously, crystals of the mixed aggregate were generated, separated from the

(29) (a) Kahn, S. D.; Keck, G. E.; Hehre, W. J. *Tetrahedron Lett.* **1987**, *28*, 279–280. (b) Keck, G. E.; Castellino, S. *Tetrahedron Lett.* **1987**, *28*, 281–284.
(30) Additional evidence is presented in Part II.
(31) Enolization of 3-pentanone by the lithium amide base **2** leads to a ratio of 32:68 = E:Z enolates in solution, whereas only the aggregate **1** containing the Z enolate isomer crystallizes preferentially from this solution.
(32) The crystallographic 2-fold rotation symmetry requirement was satisfied for the enolate by a model with the enolate oxygen atom and the carbon attached to oxygen of 3-pentanone are located on the symmetry axis. The other four carbons in the enolate residue adopt the expected conformations for 3-pentanone. Note that this symmetry of the overall aggregate **1** renders the two enolate sites virtually identical so this disorder should not adversely affect enolate enantioselectivity. This disorder is identical to that found in the crystal aggregate **4**. We note that the crystallographic disorder originally reported may be due to merohedral twinning.
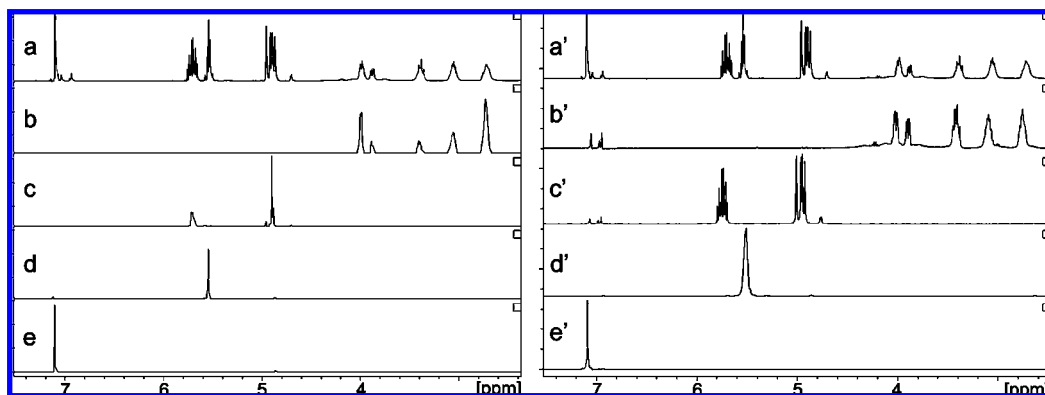
Figure 2. log D−log FW Correlation of ^{1}H (left) and ^{13}C INEPT (right) DOSY experiments of all of the species in toluene-d_8 solution.

Figure 3. Comparison between slices of ^{1}H DOSY spectra (left) with ^{1}H NMR spectra (right) of authentic samples. From top to bottom, slice or spectrum belongs to trimer **1** with internal references, trimer **1** without internal references, TDE, COE, and benzene.
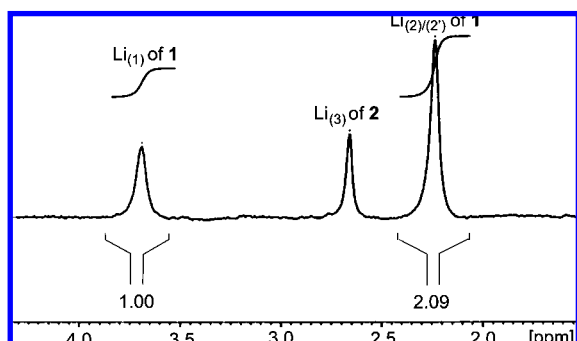

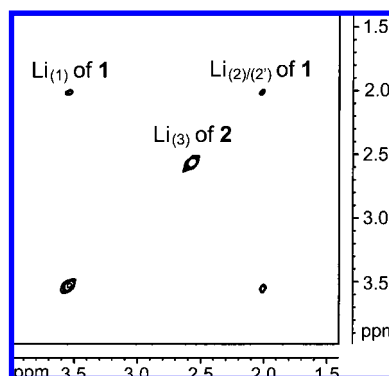**Figure 4.** ^{6}Li NMR spectrum of dissolved crystalline **1** in toluene-d_8 at −78 °C.

Figure 5. ^{6}Li−^{6}Li EXSY of dissolved crystalline **1** in toluene-d_8 at 10 °C. The mixing time of ^{6}Li−^{6}Li EXSY experiment is 4.0 s.

Figure 6. ^{6}Li−^{6}Li EXSY spectrum of toluene-d_8 solution containing aggregates **1**, **2**, and **4** at 25 °C. Cross peaks indicate intraaggregate exchange pattern. The mixing time of ^{6}Li−^{6}Li EXSY experiment is 4.0 s.

solution, dissolved in pentane, and then trapped with TMS−Cl. The TMS enol ethers obtained in this manner provided unequivocal evidence that the enolate in the crystal was (Z) and not (E); see method (a) in Scheme 3.[33] ^{1}H NMR spectrum (Figure 8, top) showed mostly *cis*-silyl enol ether and only a trace amount of trans product, the amount of which varied slightly from sample to sample.

When TMS−Cl was added immediately after the addition of 3-pentanone into the solution of Li-amide **2** in heptane, that is, without generation of the crystals, a 32:68 ratio of *E:Z* silyl enol ether was obtained as shown in Scheme 3, method (b) and Figure 8 (bottom).[34] This observation leads to the conclusion that crystal-
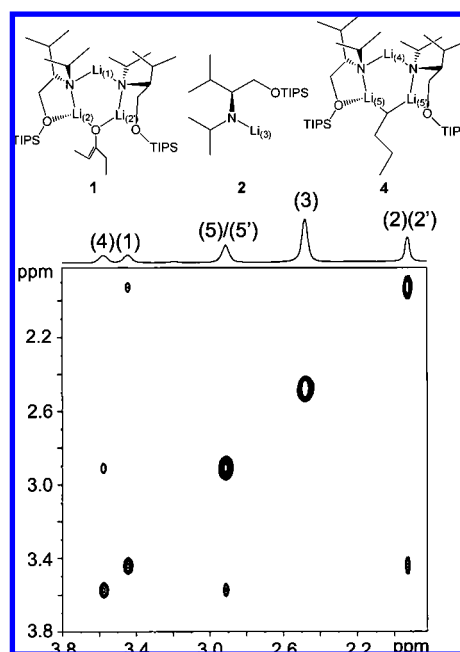
lization of the pure Z enolate-containing aggregate occurs preferentially from solution.

NMR spectroscopy is an outstanding method to study solution-state organolithium aggregates and investigate their structure−reactivity relationship. Experiments based on quadrupole coupling,[35] multiplicity and chemical exchange,[36] HMPA titration,[37] and Job plots[38] have been adapted for determining the solution structure of reactive intermediates. However, structural details, especially the aggregation state and solvation number, are always challenging to determine. In the above sections, we utilize a new NMR strategy combining diffusion-ordered NMR spectroscopy (DOSY) and 2D ^{6}Li NMR to characterize organolithium complex **1** in solution. These NMR

(33) Heathcock, C. H.; Buse, C. T.; Kleschick, W. A.; Pirrung, M. C.; Sohn, J. E.; Lampe, J. *J. Org. Chem.* **1980**, *45*, 1066−1081.

(34) For enolizations of 3-pentanone with Li-amide bases, see: (a) Sakuma, K.; Gilchrist, J. H.; Romesberg, F. E.; Cajthaml, C. E.; Collum, D. B. *Tetrahedron Lett.* **1993**, *34*, 5213−5216. (b) Kim, Y. J.; Bernstein, M. P.; Roth, A. S. G.; Romesberg, F. E.; Williard, P. G.; Fuller, D. J.; Harrison, A. T.; Collum, D. B. *J. Org. Chem.* **1991**, *56*, 4435−4439. (c) Hall, P. L.; Gilchrist, J. H.; Collum, D. B. *J. Am. Chem. Soc.* **1991**, *113*, 9571−9574. (d) Fataftah, Z. A.; Kopka, I. E.; Rathke, M. W. *J. Am. Chem. Soc.* **1980**, *102*, 3959−3960.
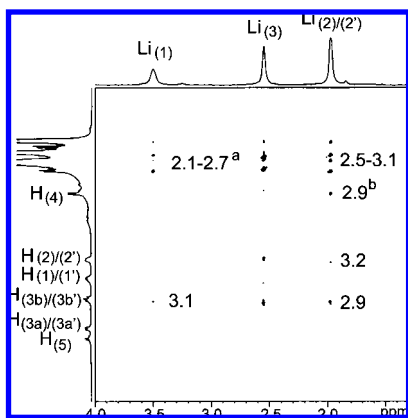
Figure 7. ⁶Li−¹H HOESY spectrum of toluene-d_8 solution containing mixed aggregate **1** and lithium amide **2** at 25 °C. (a) Spatial distance between Li and H atom, which is measured from the solid-state structure of complex **1**, is shown right of the cross peaks. (b) There is a cross peak between Li$_{(2)/(2')}$ and H$_{(4)}$, while there is no cross peak between Li$_{(2)}$ and H$_{(5)}$. These observations suggest that the 4-methyl group in the enolate is close to Li$_{(2)/(2')}$; thus the configuration of the enolate is *Z*.

Scheme 2
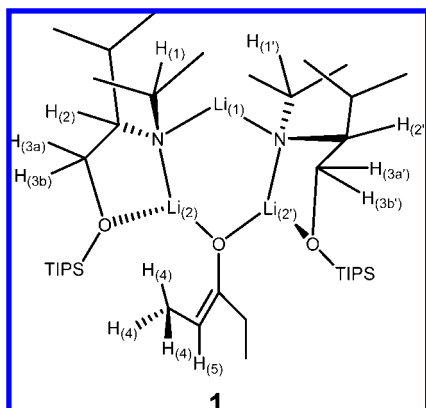
Scheme 3[a]
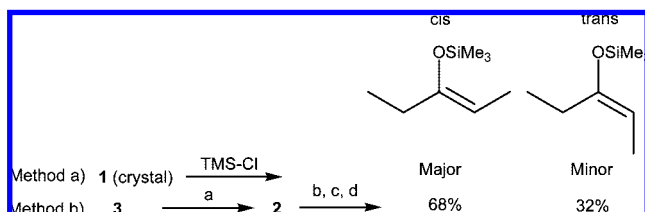
[a] (a) 1.0 equiv of 2.5 M *n*-BuLi in hexanes, heptane, 0 °C, 5 min; (b) 0.48 equiv of 3-pentanone, 0 °C, 30 min; (c) 0.48 equiv of 2.5 M *n*-BuLi in hexanes; (d) TMS−Cl.

methods can be applied to other organolithium and organometallic systems.

Part II. ⁶Li−¹H *J*-Coupling across Li−N−C−H Bonds. Observation of ⁶Li−¹H Coupling. During our ⁶Li−⁶Li EXSY

Figure 8. Part of the ¹H NMR spectrum of TMS enol ether obtained by trapping methods (a),(b) (see Scheme 3).
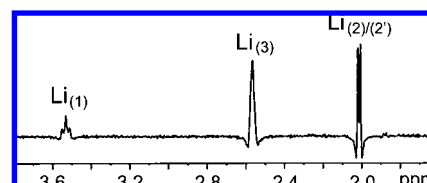
Figure 9. Proton-coupled ⁶Li NMR spectrum of solution containing mixed aggregate **1** and lithium amide **2** at −10 °C in toluene-d_8. (Sine window function applied to distinguish the couplings.)

experiments of the aggregate **1** from −25 to 25 °C, we observed ⁶Li line splitting of the lower field signal to a triplet and the higher field signal to a doublet as shown in Figure 9 in the one-dimensional ⁶Li NMR spectrum.

These splitting patterns are due to ⁶Li−¹H coupling and not to ⁶Li−⁶Li coupling, because broadband proton decoupling eliminated these observed splittings.[39] The couplings do not match the splitting pattern that is expected from ⁶Li−⁶Li coupling. One expects a quintet and a triplet of triplets for complex **1** from ⁶Li−⁶Li coupling because ⁶Li is a spin 1 nucleus. Therefore, we attribute the observed splitting to ⁶Li−¹H scalar coupling.

To the best of our knowledge, there is only one other reported example of scalar coupling between ⁶Li and ¹H and that is across

(35) (a) Jackman, L. M.; Cizmeciyan, D.; Williard, P. G.; Nichols, M. A. *J. Am. Chem. Soc.* **1993**, *115*, 6262–6267. (b) Jackman, L. M.; Chen, X. *J. Am. Chem. Soc.* **1992**, *114*, 403–411. (c) Jackman, L. M.; Bortiatynski, J. *Adv. Carbanion Chem.* **1992**, *1*, 45–87. (d) Jackman, L. M.; Scarmoutzos, L. M.; Smith, B. D.; Williard, P. G. *J. Am. Chem. Soc.* **1988**, *110*, 6058–6063. (e) Jackman, L. M.; Scarmoutzos, L. M.; DeBrosse, C. W. *J. Am. Chem. Soc.* **1987**, *109*, 5355–5361. (f) Jackman, L. M.; Szeverenyi, N. M. *J. Am. Chem. Soc.* **1977**, *99*, 4954–4962.
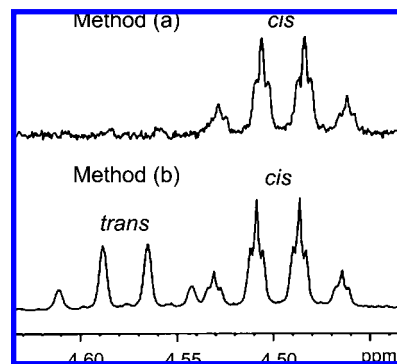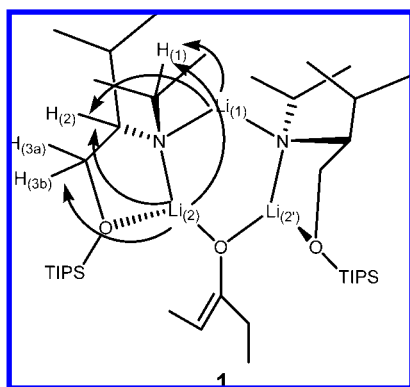
(36) (a) Fraenkel, G.; Qiu, F. *J. Am. Chem. Soc.* **2000**, *122*, 12806–12812. (b) Kim, Y.-J.; Streitwieser, A.; Chow, A.; Fraenkel, G. *Org. Lett.* **1999**, *1*, 2069–2071. (c) Fraenkel, G.; Duncan, J. H.; Martin, K.; Wang, J. *J. Am. Chem. Soc.* **1999**, *121*, 10538–10544. (d) Fraenkel, G.; Subramanian, S.; Chow, A. *J. Am. Chem. Soc.* **1995**, *117*, 6300–6307. (e) Fraenkel, G.; Martin, K. *J. Am. Chem. Soc.* **1995**, *117*, 10336–10344. (f) Fraenkel, G.; Chow, A.; Winchester, W. R. *J. Am. Chem. Soc.* **1990**, *112*, 6190–6198. (g) Fraenkel, G.; Henrichs, M.; Hewitt, M.; Su, B. M. *J. Am. Chem. Soc.* **1984**, *106*, 255–256. (h) Fraenkel, G.; Pramanik, P. *J. Chem. Soc., Chem. Commun.* **1983**, 1527–1529. (i) Fraenkel, G.; Henrichs, M.; Hewitt, J. M.; Su, B. M.; Geckle, M. J. *J. Am. Chem. Soc.* **1980**, *102*, 3345–3350. (j) Fraenkel, G.; Fraenkel, A. M.; Geckle, M. J.; Schloss, F. *J. Am. Chem. Soc.* **1979**, *101*, 4745–4747.

(37) (a) Reich, H. J.; Goldenberg, W. S.; Sanders, A. W.; Jantzi, K. L.; Tzschucke, C. C. *J. Am. Chem. Soc.* **2003**, *125*, 3509–3521. (b) Reich, H. J.; Goldenberg, W. S.; Gudmundsson, B. O.; Sanders, A. W.; Kulicke, K. J.; Simon, K.; Guzei, I. A. *J. Am. Chem. Soc.* **2001**, *123*, 8067–8079. (c) Reich, H. J.; Green, D. P.; Medina, M. A.; Goldenberg, W. S.; Gudmundsson, B. O.; Dykstra, R. R.; Phillips, N. H. *J. Am. Chem. Soc.* **1998**, *120*, 7201–7210. (d) Reich, H. J.; Gudmundsson, B. O. *J. Am. Chem. Soc.* **1996**, *118*, 6074–6075. (e) Reich, H. J.; Borst, J. P.; Dykstra, R. R.; Green, P. D. *J. Am. Chem. Soc.* **1993**, *115*, 8728–8741. (f) Reich, H. J.; Borst, J. P. *J. Am. Chem. Soc.* **1991**, *113*, 1835–1837. (g) Reich, H. J.; Green, D. P. *J. Am. Chem. Soc.* **1989**, *111*, 8729–8731.

(38) McNeil, A. J.; Collum, D. B. *J. Am. Chem. Soc.* **2005**, *127*, 5655–5661.

(39) Please refer to Figure S25 in the Supporting Information for the proton broadband decoupled spectrum.

***Scheme 4**[a]*

[a] Only possible couplings between ^{6}Li–^{1}H on the left half are shown.

Table 3. Dihedral Angles[a] between Protons and Lithium Atoms in the Crystal Structure of Complex **1**

	Li$_{(1)}$	Li$_{(2)/(2')}$
H$_{(1)/(1')}$	96.9°	163.7°
H$_{(2)/(2')}$	170.9°	87.5°
H$_{(3a)/(3a')}$		164.2°
H$_{(3b)/(3b')}$		74.2°

[a] Small J-couplings are expected for dihedral angle of about 90°; large J-couplings are expected for dihedral angle of about 0° or 180°.

Li–C–C–H bonds.[40] We find two similarities in comparing our results with those of Mons and Günther et al. First, the coupling only appears when the temperature is appropriate, that is, greater than −30 °C. These ^{6}Li–^{1}H couplings became most evident between −10 and +25 °C. We believe that this temperature effect is due to the line broadening effects due to solvent viscosity at low temperature, which prevent the observation of small line splittings. Hence, these splittings were not observed at temperature lower than −30 °C at which toluene solution becomes notably viscous. The second similarity is that the coupling constants range from $J = 0.45$ Hz for the doublet to $J = 0.89$ Hz for the triplet, values similar to those reported, that is, 0.80 Hz, for $^3J_{6\text{Li}-1\text{H}}$ coupling.[40]

From the solid-state structure of complex **1**, we conclude that the most remarkable feature of these ^{6}Li–^{1}H couplings is that they have to be transmitted either through the Li–N bond or through the Li–O coordinate bond. Although one-bond coupling directly between connected ^{6}Li–^{15}N has been observed many times,[41] we believe that this is the first reported example of ^{6}Li–^{1}H three-bond coupling transmitted through a ^{6}Li–N/O bond. Coupling through a ^{6}Li–N/O bond could account for the extremely small coupling constant. Closer examination of the structure revealed several possible protons that could couple to the lithium atoms through three bonds. As shown in Scheme 4, protons H$_{(1)}$, H$_{(2)}$ (through Li–N–C–H bonds), and H$_{(3)}$ (through Li–O–C–H bonds) could be coupled to Li$_{(2)}$, while protons H$_{(1)}$ and H$_{(2)}$ could be coupled to Li$_{(1)}$ (through Li–N–C–H bonds). Because Li$_{(2)/(2')}$ is a doublet, we conclude that it is coupled to only one proton, that is, H$_{(1)}$, H$_{(2)}$, or H$_{(3)}$. Because Li$_{(1)}$ is a triplet, we conclude that it is coupled to two protons from the ligand on each side, that is, to either H$_{(1)/(1')}$ or H$_{(2)/(2')}$.[42]

Observation of the coupling itself proves the structural integrity of this aggregate. This also implies that the dynamic processes involving the coupled protons are slow on the NMR time scale. This ^{6}Li–^{1}H coupling also provides us with the opportunity to determine stereochemical information about the

ligand relative to the lithium atoms by providing approximate dihedral angles of H–C–X–Li (X = N/O), if the magnitude of these couplings follows the Karplus-type relationship.[43,44] Dihedral angles of every possible proton relative to the two type of lithium atoms were determined from the solid-state structure, and these are listed in Table 3.

Assuming that the solution structure resembles the solid state, we suggest that protons H$_{(1)}$ and H$_{(3a)}$ are more likely to couple directly with Li$_{(2)}$ than is H$_{(2)}$ because the dihedral angles ϕ [Li$_{(2)}$–H$_{(1)}$] and ϕ [Li$_{(2)}$–H$_{(3a)}$] are both near 180°, while ϕ [Li$_{(2)}$–H$_{(2)}$] is near 90°. With respect to Li$_{(1)}$, we suggest that H$_{(2)}$ is a better candidate for the coupling because ϕ [Li$_{(1)}$–H$_{(2)}$] is very close to 180°, while ϕ [Li$_{(1)}$–H$_{(1)}$] is about 90°.

Identification of J-Coupled Protons. To assign which ^{6}Li–^{1}H interaction gives rise to the observed couplings, three separate approaches were taken. These are ^{6}Li–^{1}H HMQC spectroscopy, deuterium labeling, and selective proton decoupling experiments (Supporting Information).

a. ^{6}Li–^{1}H HMQC Spectroscopy. A ^{6}Li–^{1}H HMQC experiment was performed. Only two cross peaks between Li$_{(2)/(2')}$–H$_{(1)}$ and Li$_{(1)}$–H$_{(2)/(2')}$ were shown in the spectrum (Figure 10). We can conclude that H$_{(1)}$ is the only proton coupled to Li$_{(2)}$. This conclusion excludes the possibility of H$_{(2)}$–Li$_{(2)}$ and H$_{(3)}$–Li$_{(2)}$ coupling. Also, H$_{(2)}$ as well as H$_{(2')}$ (the equivalent of H$_{(2)}$ on the other side of the aggregate) are responsible for the splitting of Li$_{(1)}$ into a triplet, and no scalar coupling is observed between Li$_{(1)}$–H$_{(3)}$ and Li$_{(2)}$–H$_{(3)}$. The cross peaks contain complicated substructures, which provide coupling constants and other useful information as previously shown by Günther et al.[40] Coupling constants extracted from the HMQC spectrum agree qualitatively with those determined by ^{6}Li NMR in Figure 9.

b. Deuterium Labeling Experiments. To prove unambiguously the origin of these couplings, we prepared deuterium-labeled samples. Thus, two deuterated derivatives of ligand **3**, shown in Scheme 5 as **3**(3D) and **3**(2D), were prepared according to the literature procedures for preparation of

(40) Mons, H. E.; Günther, H.; Maercker, A. *Chem. Ber.* **1993**, *126*, 2747–2751.

(41) (a) Carlier, P. R.; Lucht, B. L.; Collum, D. B. *J. Am. Chem. Soc.* **1994**, *116*, 11602–11603. (b) Bauer, W.; Schleyer, P. v. R. *Adv. Carbanion Chem.* **1992**, *18*, 89–175. (c) Gilchrist, J. H.; Collum, D. B. *J. Am. Chem. Soc.* **1992**, *114*, 794–795. (d) DePue, J. S.; Collum, D. B. *J. Am. Chem. Soc.* **1988**, *110*, 5518–5524. (e) Galiano-Roth, A. S.; Michaelides, E. M.; Collum, D. B. *J. Am. Chem. Soc.* **1988**, *110*, 2658–2660. (f) Kallman, N.; Collum, D. B. *J. Am. Chem. Soc.* **1987**, *109*, 7466–7472.

(42) Williard, P. G.; Sun, C. *J. Am. Chem. Soc.* **1997**, *119*, 11693–11694.

(43) (a) Karplus, M. *J. Chem. Phys.* **1959**, *30*, 11–15. (b) Karplus, M. *J. Am. Chem. Soc.* **1963**, *85*, 2870–2871.

(44) For examples of structure interpretation utilizing Karplus-type relationship of heteronuclear ^5J coupling such as ^5J(Sn, C) through Sn–C–C–C bonds [(h), (b)], ^5J(Sn, H) through Sn–C–C–H bonds [(g), (b)], ^5J(Sn, Si) through Sn–C–C–Si bonds (d), and ^5J(Sn, Sn) through Sn–C–C–Sn bonds (d), see: (a) Ma, K.; Rettig, S. J.; James, B. R. *Chem. Commun* **1999**, *24*, 2463–2464. (b) Mitchell, T.; Podesta, J. C.; Ayala, A.; Chopa, A. B. *Magn. Reson. Chem.* **1998**, *26*, 497–500. (c) Thibaudeau, C.; Plavec, J.; Chattopadhyaya, J. *J. Org. Chem.* **1998**, *63*, 4967–4984, and ref 9 therein. (d) Mitchell, T.; Kowall, B. *Magn. Reson. Chem.* **1995**, *33*, 325–328. (e) Plavec, J.; Chattopadhyaya, J. *Tetrahedron Lett.* **1995**, *36*, 1949–1952. (f) Zerbe, O.; Pountney, D. L.; Vonphilipsborn, W.; Vasak, M. *J. Am. Chem. Soc.* **1994**, *116*, 377–378. (g) Quintard, J. P.; Degeuil-Castaing, M.; Barbe, B.; Petraud, M. *J. Organomet. Chem.* **1982**, *234*, 41–61. (h) Doddrell, D.; Burfitt, I.; Kitching, W.; Bullpitt, M.; Lee, C. H.; Mynott, R. J.; Considine, J. L.; Kuivila, H. G.; Sarma, R. H. *J. Am. Chem. Soc.* **1974**, *96*, 1640–1642.
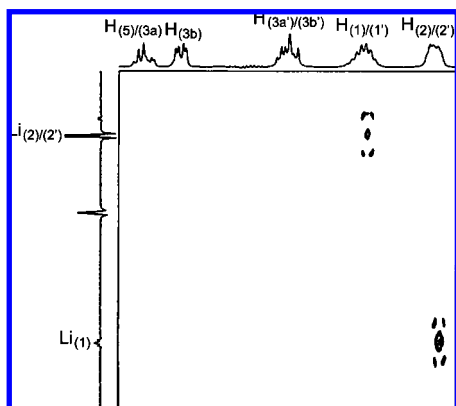
Figure 10. ^{6}Li$-^1$H HMQC spectrum of toluene-d_8 solution containing mixed aggregate **1** and lithium amide **2** at 25 °C.

compound **3** where NaCNBD$_3$ and LiAlD$_4$ were used instead of NaCNBH$_3$ and LiAlH$_4$, respectively.[21]

The deuterium-labeled compounds **3**(3D) and **3**(2D) were then used to generate the corresponding enolate containing mixed aggregates **1**(3D) and **1**(2D) shown in Scheme 6, which were used to repeat the ^{6}Li NMR experiments described in Supporting Information Figure S25. The NMR results are shown in Figure 11.

The ^{6}Li spectrum of **1**(3D), shown in Figure 11a, was as expected in that the doublet for Li$_{(2)}$ turned into a singlet while the triplet for Li$_{(1)}$ remained. Clearly, one of the protons at the H$_{(1)}$ or H$_{(3)}$ position contributed to the coupling of Li$_{(2)}$, while H$_{(2)}$ definitely was responsible for the coupling to Li$_{(1)}$. The ^{6}Li spectrum of **1**(2D), shown in Figure 11c, was the same as nonlabeled sample. Hence, we have completely and unambiguously confirmed that only H$_{(1)}$ is coupled to Li$_{(2)}$.

All of the above evidence clearly supports our conclusion that the structure of the aggregate **1** retains a very similar stereostructure in solution as in the solid state. The aggregate **1** appears to be comparatively stable in solution. We conclude that the N$-$Li$_{(2)}$/N$-$Li$_{(2')}$ bond is fairly strong because we observe H$_{(1)}-$Li$_{(2)}$ coupling through H$-$C$-$N$-$Li bonds. The absence of the H$_{(3)}-$Li$_{(2)}$ coupling is not easily explained, but we suggest that it may be absent either because of the NMR opaque nature of the Li$-$O coordination bond or because the O$-$Li$_{(2)}$/O$-$Li$_{(2')}$ coordination is relatively weak.

The rare observation of the ^{6}Li$-^1$H coupling is perhaps not fortuitous. The fact that this coupling has not been commonly observed may be a consequence of the relatively small *J* value. Extensive use of proton decoupling in ^{6}Li NMR is common to obtain sharper lines in the ^{6}Li spectrum. Such proton decoupling precludes observation of the ^{6}Li$-^1$H *J*-coupling. The latter point itself is a strong piece of evidence that the Li$-$H coupling generally exists. We believe that two factors generally make it difficult to observe ^{6}Li$-^1$H coupling, that is, the broad ^{6}Li line width at lower temperature and the rapid intermolecular exchange and/or the existence of different aggregates at higher temperature. In the above ^{6}Li NMR investigations of complex **1**, both of the two factors were avoided, and thus we observed this unique Li$-$N$-$C$-$H three-bond coupling, which gave valuable stereochemical information of complex **1**.

Conclusions

While X-ray crystallographic methods are most widely used for solid-state structure determination, questions remain concerning the relationship of solid-state structures of organolithium

reagents with those in solution. A relevant question concerning the structural integrity of organolithium reagents in these two very different phases is whether the structure determined in the solid state represents the only, the major, or one among several species in the solution. Also, it is of considerable interest to determine which, if any, of these structures participate in reactions that these reagents undergo. One must also ask whether and how easily the stereostructure changes in solution relative to solid state. Therefore, solution structure determination represents a critical complement to X-ray structure determination of organolithium aggregates. In the above sections, we prove the solution-state structure of complex **1** is similar to the solid-state structure; however, the stereochemistry of the enolate double bond is dependent on reaction conditions. These observations also lend credence to our hypothesis that chiral aggregate **1** is the major observable nucleophile in solution and likely to play a key role in the enantioselective aldol reaction when aldehydes are added to this solution.

In the present article, we report a detailed analysis of the solution structure of mixed complex **1** using the combined methods of DOSY and 2D ^{6}Li NMR techniques. Our results include ^{1}H and ^{13}C INEPT DOSY at 25 and -78 °C to prove the aggregation state, ^{6}Li$-^6$Li EXSY as evidence of an intramolecular-only exchange pattern in this aggregate, and ^{6}Li$-^1$H HOESY experiment to confirm the stereochemical structure of the chiral aggregate. We also investigate the stereochemistry of the enolate in complex **1**, and these observations are helpful for the application of this chiral enolate complex in the stereoselective carbon$-$carbon formation reactions.

Furthermore, a unique ^{6}Li$-^1$H coupling through Li$-$N$-$C$-$H network was discovered, and the stereo origin of this coupling was confirmed by selective proton decoupling ^{6}Li NMR experiments, ^{6}Li$-^1$H HMQC spectroscopy, and making deuterium-labeled compounds. These observations provide very useful information of the stereostructure of the protons on ligand relative to the lithium atoms in complex **1**.

Experimental Section

General. All NMR samples were directly prepared in the NMR tubes. All NMR tubes were sealed with septa and then flame-dried under vacuum and filled with argon before use. Toluene-d_8 was kept with 4 Å molecular sieves under argon. *n*-BuLi was obtained as 2.5 M in hexanes, and the exact concentration of the solution was determined by titration with diphenyl acetic acid in THF. NMR experiments in Figures 4$-$11 were recorded on a 300 MHz spectrometer with a variable-temperature unit unless otherwise noted. Measuring frequencies were 300.13 MHz (^{1}H), 75.47 MHz (^{13}C), and 44.17 MHz (^{6}Li). All other NMR experiments were recorded on a 400 MHz spectrometer with a variable-temperature unit. Standard ^{1}H and ^{13}C NMR spectra were recorded at 400.13 and 100.61 MHz, respectively. All ^{13}C spectra are proton decoupled. ^{1}H and ^{13}C chemical shifts were referenced to the toluene-d_8 signals at δ 2.08 ppm and 20.4 ppm, respectively, in toluene-d_8.

DOSY Experiments. DOSY experiments were performed on a 400 MHz spectrometer equipped with an *z*-axis gradient amplifier and a probe with a *z*-axis gradient coil. Maximum gradient strength was 0.214 T/m. Bipolar rectangular gradients were used with total durations of 0.5$-$3 ms. Gradient recovery delays were 0.5$-$1 ms. Diffusion times were between 500 and 2000 ms. Individual rows of the quasi-2-D diffusion databases were phased and baseline corrected.

^{6}Li NMR Experiments. Measuring frequencies for ^{6}Li NMR was 44.17 MHz. ^{6}Li spectra were referenced to external 0.3 M ^{6}LiCl in MeOH-d_4 set at δ 0.0 ppm. The mixing time of ^{6}Li$-^6$Li EXSY experiment is 4.0 s.[15b] For ^{6}Li$-^1$H HMQC experiment, the

Scheme 5

Scheme 6

3(2D) X=H   **1**(2D) X=H
3(3D) X=D   **1**(3D) X=D
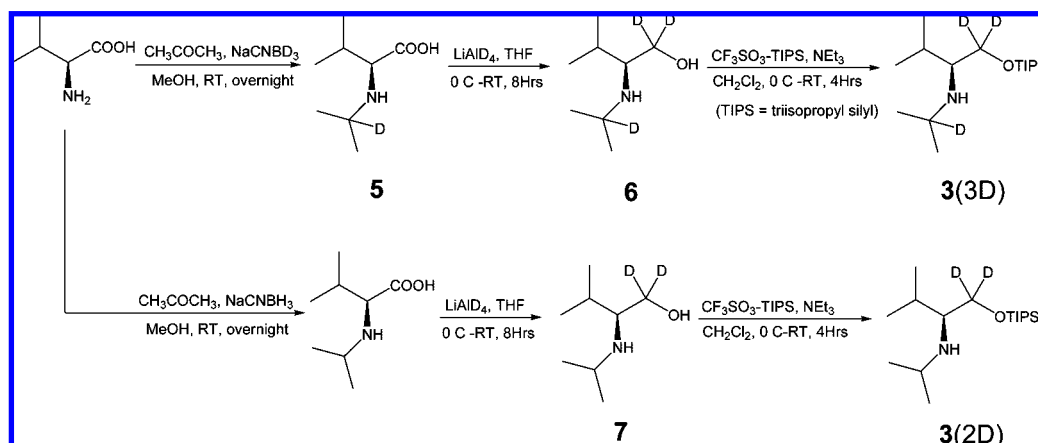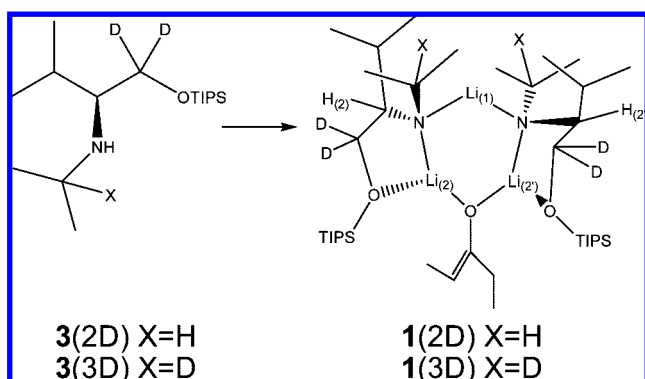
delay time between the ^{1}H-90° and the ^{6}Li-90° pulse was set at 250 ms, which is approximately $1/6J$ ($J = 0.67$ Hz is the average of the two observed ^{1}H–^{6}Li coupling constants) following the literature precedent.[40]

Synthesis of Chiral Amino Ether Ligand (3). The synthetic route adopted to prepare chiral amino ether ligands **3** started from
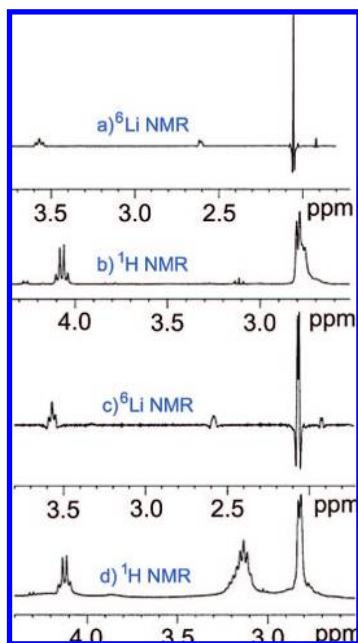

Figure 11. ^{6}Li (a and c) and ^{1}H NMR (b and d) spectra of toluene-d_8 solution containing mixed aggregate **1**(3D) (a and b) and **1**(2D) (c and d) and corresponding lithium amide **2** at −10 °C.

enantiomerically pure L-valine. The amino group was condensed with acetone to afford the corresponding imine, and reduced with sodium cyanoborohydride.[21] The *N*-isopropyl valine was subsequently reduced into the desired amino alcohol using lithium aluminum hydride. Ligand **3** was prepared from amino alcohol using triisopropylsilyl triflate as a silylation reagent and triethyl amine as a base. The deuterium-labeled ligand was prepared in a similar way.

Preparation of NMR Samples. A sample of aggregate **1** in toluene-d_8 was generated by slow addition of 3-pentanone into a solution of Li-amide **2** followed by regenerating the Li-amide ligand as depicted in Scheme 1. Thus, 1 mmol of 2.5 M *n*-BuLi in hexane was added via syringe into a Schlenk tube under argon stoppered with a rubber septum containing 2 mL of toluene-d_8 and 1 mmol of amine **3** that was chilled in an ice bath. After 5 min of stirring, 0.55 mmol of 3-pentanone were then added slowly via syringe over 30 min. After another 5 min of stirring, 0.55 mmol of *n*-BuLi was added to regenerate Li-amide. ^{1}H NMR, ^{13}C NMR, COSY, HSQC, HMBC experiments of complex **1** were carried out. Next, 0.2 M TDE, 0.2 M COE, and 0.033 M benzene was added to the above sample as internal references for DOSY experiments.

Deuterium-Labeled Samples. {1-D}-(*S*)-*N*-isopropyl-valine (**5**): ^{1}H NMR (CD$_3$OD, 300 MHz) δ 3.33 (1H, d, $J = 4.3$ Hz), 2.12 (1H, m), 1.25 (6H, d, $J = 15.6$ Hz), 1.00 (6H, dd, $J = 9.3$, 7.0 Hz); ^{13}C NMR (CD$_3$OD, 75 MHz) δ_c 174.8, 67.5, 31.4, 20.8, 19.3, 19.1, 18.9; HRMS (CI, iso-butane) calcd for [C$_8$H$_{16}$NO$_2$D + H]$^+$ 161.1400, found 161.1405.

{3-D}-(*S*)-*N*-isopropyl-valinol (**6**): ^{1}H NMR (CDCl$_3$, 300 MHz) δ 2.44 (1H, d, $J = 6.0$ Hz), 1.76 (1H, m), 1.05 (6H, d, $J = 12.3$ Hz), 0.92 (6H, dd, $J = 19.2$, 6.9 Hz); ^{13}C NMR (CDCl$_3$, 75 MHz) δ_c 61.0, 60.1 (quint. $J_{CD} = 21.44$ Hz), 46.0 (t, $J_{CD} = 20.37$ Hz), 29.7, 23.6, 23.3, 19.5, 18.3; HRMS (CI, iso-butane) calcd for [C$_8$H$_{16}$NOD$_3$ + H]$^+$ 149.1733, found 149.1729.

{2-D}-(*S*)-*N*-isopropyl-valinol (**7**): ^{1}H NMR (CDCl$_3$, 300 MHz) δ 2.89 (1H, sept., $J = 6.3$ Hz), 2.44 (1H, d, $J = 6.0$ Hz), 1.76 (1H, m), 1.05 (6H, dd, $J = 11.3$, 6.3 Hz), 0.92 (6H, dd, $J = 17.6$, 7.0 Hz); ^{13}C NMR (CDCl$_3$, 75 MHz) δ_c 61.0, 60.1 (quint. $J_{CD} = 21.44$ Hz), 46.4, 29.5, 23.6, 23.3, 19.4, 18.2; HRMS (CI, iso-butane) calcd for [C$_8$H$_{17}$NOD$_2$ + H]$^+$ 148.1600, found 148.1601.

{3-D}-(*S*)-*N*-isopropyl-*O*-triisopropylsilyl-valinol (**3**(3D)): ^{1}H NMR (CDCl$_3$, 300 MHz) δ 2.38 (1H, d, $J = 5.4$ Hz), 1.82 (1H, m), 1.12−1.01 (27H, m), 0.91(6H, dd, $J = 6.9$, 1.3 Hz); ^{13}C NMR (CDCl$_3$, 75 MHz) δ_c 62.4 (quint. $J_{CD} = 21.44$ Hz), 61.6, 46.2 (t, $J_{CD} = 20.37$ Hz), 29.2, 23.5, 23.4, 18.9, 18.7, 18.0, 12.0; HRMS (CI, iso-butane) calcd for [C$_{17}$H$_{37}$NOSiD$_3$ + H]$^+$ 305.3067, found 305.3068.

{2-D}-(*S*)-*N*-isopropyl-*O*-triisopropylsilyl-valinol (**3**(2D)): ^{1}H NMR (CDCl$_3$, 300 MHz) δ 2.84 (1H, m), 2.38 (1H, d, $J = 5.4$ Hz), 1.82 (1H, m), 1.12−1.01 (27H, m), 0.91(6H, dd, $J = 6.9$, 1.3 Hz); ^{13}C NMR (CDCl$_3$, 75 MHz) δ_c 62.4 (quint. $J_{CD} = 21.44$ Hz),

61.6, 46.7, 29.2, 23.64, 23.56, 18.9, 18.7, 18.0, 12.0; HRMS (CI, iso-butane) calcd for $[C_{17}H_{38}NOSiD_2 + H]^+$ 304.3005, found 304.3000.

Supporting Information Available: ^{1}H NMR and ^{13}C NMR spectra of ligand **3** and ^{1}H NMR, ^{13}C NMR, COSY, HSQC, HMBC, ^{1}H DOSY, and ^{13}C INEPT DOSY spectra and selective proton decoupling [6]Li NMR experiments of complex **1**. This material is available free of charge via the Internet at http://pubs.acs.org.

JA802114J